C.P. No. 1286

C.P. No. 1286

PROCUREMENT EXECUTIVE, MINISTRY OF DEFENCE

AERONAUTICAL RESEARCH COUNCIL

CURRENT PAPERS

Some Predictions Of Crack Propagation Under Combined Cabin Pressurisation And Acoustic Loadings

by

W. T. Kirkby

Structures Dept., R.A.E., Farnborough

LONDON: HER MAJESTY'S STATIONERY OFFICE

1974

PRICE 50p NET

UDC 629.13.013.1/2 : 629.13.067.4 : 539.219.2 :
539.831 : 539.433 : 534.1

CP No.1286*
January 1973

SOME PREDICTIONS OF CRACK PROPAGATION UNDER COMBINED CABIN PRESSURISATION AND ACOUSTIC LOADINGS

by

W. T. Kirkby

SUMMARY

Predictions are made of the contributions that acoustic loading and pressurisation cycling may make to the growth of a longitudinal crack in the pressure cabin of an aircraft. The results of the analysis show that the contribution to crack growth from the acoustic loading may exceed the contribution from pressurisation cycling, even though the acoustic loading alone is not sufficiently severe to initiate fatigue damage.

It may be necessary therefore to make allowance for acoustic loading when establishing the fail safe characteristics of such structure and of other areas of structure where fail safe considerations apply.

Simplifying assumptions are made in the analysis and there is need for experimental studies to substantiate the above predictions.

---

* Replaces RAE Technical Report 73004 - ARC 34641

CONTENTS

1 INTRODUCTION

In establishing the airworthiness of fail safe structures it is necessary[1] to demonstrate that any fatigue cracks that may occur will not grow to catastrophic proportions before detection and subsequent remedial action. To establish whether this requirement is met, the full scale fatigue test* on such a structure will generally include observation of the growth rates of any cracks in the structure ('natural' or artificially induced) and such observations will subsequently be related to the frequency of inspection of the structure in service.

The particular nature of the loads applied to the structure during the full scale test will depend on the intended usage of the aircraft. The intention is that all the significant loading actions - such as the ground-air-ground cycle, cabin pressurisation load and manoeuvre loads - which individually, or together, may promote fatigue damage shall be adequately represented in the test. However, because of the resultant complexity of the tests, it is not practicable to represent faithfully all of the secondary loadings and other environmental conditions, such as temperature effects, humidity and corrosion, which may arise in service and which may advance or retard the growth of fatigue damage. Exceptionally, if it is believed that some particular aspect of the environment will contribute damage on a scale comparable with the major fatigue loading actions then, of course, the additional cost and complexity must be faced - an example of this is the application of heat in the Concorde test. Generally, however, the effects of such environmental conditions are covered by appropriate safety factors.

One of the loading actions not included in the full scale test is the acoustic loading associated with jet efflux. Generally, this loading action is of significance only during engine ground running at maximum power and during take-off - nevertheless, it may be an important design consideration for the surfaces of structure which lie aft of the engine efflux nozzles. The pressure fluctuations associated with the acoustic field give rise to very large numbers of stress cycles - greater than 10^9 cycles in the life of an aircraft - of relatively low stress amplitudes. The stress amplitude varies in a random manner and, in a typical design situation may have an average value (root mean square) of about 10-20% of the 1g stress level for the aircraft. In recent

---

* Such full scale tests may be carried out on a complete airframe or on major components.

years design methods have been evolved[2] for predicting the fatigue life of surface structure under this loading action. The intention in design is that acoustic fatigue failure will not occur within the life of the aircraft (i.e. a safe-life approach to this particular problem is adopted) and tests on appropriate components are carried out to confirm the soundness of the design, using sirens to simulate the acoustic environment. However, assuming that the above design and test procedure has been followed and an adequate acoustic fatigue life has been demonstrated, there remains a further possibility that cannot be ignored when considering the overall airworthiness of a structure which, with respect to the other loading actions, is designed on fail safe principles. This possibility is that the acoustic fatigue loading action may accelerate the growth of cracks in surface structure which have been induced by the other loading actions. If this is so, then allowance must be made for the contribution made by the acoustic loads to crack growth when establishing fail safe characteristics of the structure.

In order to put this potential problem in focus a practical case has been examined - the problem of crack growth in the skin of a pressure cabin under combined pressurisation and acoustic loading. Estimates are made of the contributions to a growing crack arising from the cabin pressurisation stress cycles, from the acoustic fatigue stress cycles, and also of crack growth under a combination of the two loading actions. A very simple representation is used of the true situation which is extremely complex. The results obtained from this simplified analysis indicate that, over a typical inspection period, the crack growth associated with the combination of acoustic and cabin pressurisation loadings may be many times greater than that arising from cabin pressurisation alone. This is an important finding in relation to the fail safe behaviour of the pressure cabin structures and the same considerations may apply to other areas of the structure exposed to acoustic excitation, e.g. fin and tail plane structure, which may be designed on fail safe principles to withstand the appropriate gust and manoeuvre fatigue load spectra.

2 THE MODEL CONSIDERED

The analysis which follows is centred on the behaviour of a longitudinal crack in one panel of a pressure cabin. The panel is regarded as being flat and is bounded by frames and stringers; it is assumed that the stringer is bonded to the skin and that the crack runs close to the edge of the stiffener - see Fig.1.

Under pressure cabin cycling it is assumed that the crack is subjected to uniaxial in-plane (hoop) stress, the stress field lying normal to the crack; the

longitudinal stress field is not included as it will not have a significant effect on the growth rate of the crack[3]. It is assumed, as in the general design procedure[2], that under the acoustic fatigue loading action the panel is responding in its fundamental mode so that reversed bending stresses are induced along the boundaries. The acoustic loading is regarded as being significant only during engine ground running at maximum power and during take-off because the associated sound pressure level falls off rapidly as the aircraft gains forward speed. Thus, for each flight, the crack grows under many cycles of reverse bending associated with the acoustic loads followed by one cycle of in-plane loading representing the cabin pressurisation cycle.

3 SOME DETAILS OF THE STRESS CONDITIONS IN THE PANEL

3.1 The acoustic fatigue stress spectrum

The stress spectrum under the acoustic loading action is assumed, as in design, to approximate to a Rayleigh distribution of peak amplitude, i.e. the probability of having a stress peak between f and $(f + \delta f)$ is given by

$$P(f)df = \frac{f}{\sigma^2} e^{-(f^2/2\sigma^2)} df \qquad (1)$$

where σ = root mean square (rms) stress,

f = stress level.

Figs.2a and 2b show a typical stress/time waveform and illustrate the distribution. Theoretically this distribution applies up to values of $f/\sigma = \infty$; in practice the distribution will be truncated in the vicinity of $f/\sigma = 4$.

The rms stress levels used in representing the acoustic fatigue stresses are taken from consideration of the probable bending stresses at the panel boundary if the RAeS/ESDU design procedure[2] is followed in order to obtain freedom from failure within the lifetime of the aircraft. It may be seen from the associated data sheets that a life considerably greater than 10^9 cycles, which is adequate in terms of the aircraft life, will be obtained if average bending stress (σ) at the boundary is less than 10 MN m^{-2} ($\approx$ 1.45 ksi) root mean square - as exemplified in Figs.3a and 3b. It should be mentioned in passing that this value of stress takes into account the stress concentration effect in the absence of a crack when the skin 'bends over the edge' of the stiffener. In the subsequent analysis in this Report (section 5) results are given for a range of rms values of stress between 5 and 10 MN m^{-2} ($\approx 0.725 \rightarrow 1.45$ ksi).

For the purposes of calculating the number of acoustic stress cycles N_{ac} experienced in each flight it is assumed, as in design, that the ground running together with the take-off period (total, t) averages 90 seconds per flight. The fundamental frequency (ω) of a panel in a pressure cabin will commonly lie in the range 150-250 Hz, and in the predictions which follow a frequency of 200 Hz is assumed - thus the number of cycles per flight, N_{ac}, associated with the acoustic loading is given by

$$N_{ac} = \omega t = 1.8 \times 10^4 \text{ cycles} \quad .$$

The above considerations of the acoustic fatigue loading and response of the panel are based on the behaviour of an uncracked panel. The behaviour of a cracked panel in an acoustic field is extremely complex and forms the subject of current research investigations. As the crack grows along one boundary of the panel the fundamental frequency of the panel will fall somewhat and the mode shape will change. However, the frequency bandwidth of the acoustic excitation is relatively broad and there is no reason to believe that the overall panel response to the excitation will diminish. In this Report, it is assumed that the average rms bending stresses in the path of the growing crack remain constant.

3.2 The cabin pressurisation stress cycle

The loading action under cabin pressurisation is assumed to give rise to an axial in-plane stress cycle, $0\text{-}S_p\text{-}0$, where S_p is the pressure cabin hoop stress and is taken in the worked examples (section 5) to lie between 70 MN m^{-2} and 100 MN m^{-2} ($\approx$ 10 ksi to 14.5 ksi). One cycle of such loading occurs per flight.

4 THE CRACK GROWTH ANALYSIS

In the analysis which follows fracture mechanics principles are applied to the prediction of crack growth under the two loading actions considered. Much of the detailed analysis is based on work by Roberts and Erdogan[4] who established a relationship by which crack growth under reversed bending conditions can be deduced from crack growth data obtained under axial loading conditions - this relationship is discussed in section 4.1 below. In section 4.2 below an expression is derived from which crack growth in bending may be predicted, under a Rayleigh distribution of peak amplitudes, from crack growth data[5] obtained under in-plane loading of constant amplitude waveform.

Subsequently, in section 4.3, an expression is derived with which crack growth under the cabin pressurisation cycle can be predicted using the same body of data[5]. The two expressions describing crack growth behaviour under acoustic excitation alone and under cabin pressurisation alone are combined in section 4.4 to derive an expression for the prediction of crack growth under a combination of the two loading actions. Finally, in section 4.5, simplified expressions are derived for predicting the relative crack growth rates under the three differing loading cases discussed above.

4.1 Crack propagation under axial loading and under reversed bending

Roberts and Erdogan[4] put forward an equation of the following form to fit crack growth data in a panel subjected to uniaxial stress cycling:-

$$\text{For axial loading } \frac{da}{dN} = C_1 C_2^{(m+p)} k_{max}^{m} \Delta k^{p} \qquad (2)$$

where a = half crack length

N = number of cycles

$k_{max} = f_{max}\sqrt{a}$ (f_{max} being the maximum gross stress in the cycle)

$\Delta k = (f_{max} - f_{min})\sqrt{a}$ (f_{min} being the minimum gross stress in the cycle)

C_1, m and p are constant for the material concerned and are obtained empirically

C_2 is a constant introduced to correct for the structural geometry in the vicinity of the crack and is obtained by analysis. It may, for instance, include finite width corrections.

For crack propagation under reversed bending Roberts and Erdogan[4] proposed the introduction of a further constant, λ, based on considerations of plastic zone size at the crack tip under bending as opposed to axial loading, thus:-

$$\text{For reversed bending } \frac{da}{dN} = C_1 C_2^{(m+p)} \lambda^{(m+p)} k_{max}^{m} \Delta k^{p} \quad . \qquad (3)$$

The authors derived empirical values of λ lying between 0.44 and 0.502 over a wide range of Δk with $R = -1$*, and using a range of sheet thicknesses between 1.25 mm and 4 mm (0.050 in and 0.16 in). In subsequent worked examples a value of $\lambda = 0.5$ is taken. It will be noted that in this analysis C_2 is used for both axial and bending conditions - this is discussed in the concluding paragraph of section 4.4 below.

---

* R = minimum stress in the cycle/maximum stress in the cycle.

4.2 Crack growth under acoustic loading

In this section an expression is derived for predicting crack growth in reversed bending under acoustic loading. A modification is first made to equation (3) to obtain compatibility with the presentation adopted by Hudson[5] in giving data for 2024-T3 sheet material. The latter data were obtained under axial loading for a range of stressing conditions, covering stress ratios from $R = -1$ to $R = +0.8$. In Hudson's analysis, under $R = -1$ conditions Δk is taken to be associated with the positive range of stress (i.e. $f_{max} - f_{zero}$). With this modification equation (3) may be written:-

$$\frac{da}{dN} = C_1 C_2^n \lambda^n \Delta k^n \tag{4}$$

where $n = m + p$.

Expressing Δk in terms of crack length a and a positive stress range f gives:-

$$\frac{da}{dN} = C_1 C_2^n \lambda^n a^{n/2} f^n \tag{5}$$

Thus, under a Rayleigh distribution of peak stresses (equation (1)), and assuming simple summation of increments of crack growth associated with each stress cycle in the spectrum, the average crack growth rate is given by

$$\frac{da}{dN} = C_1 C_2^n \lambda^n a^{n/2} \int_0^\infty f^n P(f) df \tag{6}$$

Equation (6) may be written (see Appendix A)

$$\frac{da}{dN} = C_1 C_2^n \lambda^n a^{n/2} (2\sigma^2)^{n/2} \Gamma\left(\frac{n}{2} + 1\right) \quad . \tag{7}$$

In practice an incomplete gamma function should be substituted for $\Gamma\left(\frac{n}{2} - 1\right)$ in equation (7). This is because, for a given crack length, there will be a threshold value of f below which crack growth will not occur [corresponding to a threshold value[6] of $C_2 f \sqrt{\pi a} = 1.65$ MN $m^{-3/2}$ (1500 lb $in^{-3/2}$)].

Also, as mentioned in section 3.1 above, the Rayleigh distribution will be truncated at an upper value of $f/\sigma = 4$. Then equation (7) may be modified to read:-

$$\frac{da}{dN} = C_1 C_2^n \lambda^n a^{n/2} (2\sigma^2)^{n/2} \Gamma_{x \to y}\left(\frac{n}{2} + 1\right) \tag{8}$$

where $x = \frac{f_{th}^2}{2\sigma^2}$, and $y = 8$ (corresponding to $\frac{f^2}{2\sigma^2}$ for $\frac{f}{\sigma} = 4$) and f_{th} is the threshold value of f for a crack of length a. Values of $\Gamma_{x \to y}\left(\frac{n}{2} + 1\right)$ covering the range of this analysis are given in Table 1. From equation (8) it can be shown that the resultant crack length a_2, following the application of N_{ac} stress cycles of the Rayleigh distribution with a crack of original length a_1, is given by

$$a_2 = \left[a_1^{\left(1 - \frac{n}{2}\right)} + C_1 C_2^n \lambda^n \left(1 - \frac{n}{2}\right) (2\sigma^2)^{n/2} \Gamma_{x \to y}\left(\frac{n}{2} + 1\right) N_{ac}\right]^{\frac{1}{\left(1 - \frac{n}{2}\right)}} \tag{9}$$

4.3 Crack growth under cabin pressurisation cycling

In the prediction of crack growth rate under the cabin pressurisation cycle equation (2) may be used. Again, it will be noted that $k_{max} = \Delta k$ $(R = 0)$, hence

$$\frac{da}{dN} = C_1 C_2^n \Delta k^n \tag{10}$$

where $n = m + p$.

Then expressing Δk in terms of crack length a and cabin pressurisation stress S_p, gives:

$$\frac{da}{dN} = C_1 C_2^n a^{n/2} S_p^n \quad . \tag{11}$$

From this equation it may be shown that the resultant crack length a_2 following the application of N_p pressurisation cycles with a crack of original length a_1, is given by

$$a_2 = \left[a_1^{\left(1 - \frac{n}{2}\right)} + C_1 C_2^n S_p^n \left(1 - \frac{n}{2}\right) N_p\right]^{\frac{1}{\left(1 - \frac{n}{2}\right)}} \tag{12}$$

4.4 Crack growth under a combination of cabin pressurisation and acoustic loading

In the discussion of the analytical model (section 2) it was indicated that the acoustic and cabin pressurisation loading actions occur sequentially, rather than together, i.e. that stresses arising from acoustic excitation are not superimposed on the cabin pressurisation stress. Equation 9 and equation 12 may then be summed to give an expression for crack growth under the combined loading actions; *viz*

$$a_2 = \left[a_1^{\left(1 - \frac{n}{2}\right)} + C_1 C_2^n \left\{ S_p^n \left(1 - \frac{n}{2}\right) N_p + \lambda^n \left(1 - \frac{n}{2}\right) (2\sigma^2)^{n/2} \Gamma_{x \to y} \left(\frac{n}{2} + 1\right) N_{ac} \right\} \right]^{\frac{1}{\left(1 - \frac{n}{2}\right)}} \quad \ldots\ldots (13)$$

It may be noted that in obtaining this expression for the overall crack growth rate, equation (13), no allowance is made for any stress interaction effects that may occur under a combination of both forms of loading. On first consideration it might be assumed that the tensile stress cycle associated with the cabin pressurisation would significantly retard crack growth under the acoustic fatigue stress history which, in terms of rms stress is much less severe. However it must be remembered that the acoustic loading, which occurs under zero mean stress conditions, gives rise to a spectrum of positive and negative stress peaks the largest of which reach some four times the rms level. Insofar as interaction effects during crack propagation are understood, it seems likely that the negative stress excursions, which are experienced under acoustic loading between each cabin pressurisation cycle, will tend to suppress the retardation effects which would otherwise arise from the (tensile) pressurisation peaks. Current experimental research studies will shed further light on this problem.

4.5 The relative crack propagation rates under acoustic loading, under pressurisation loading, and under a combination of both loadings

It will be recollected from the observations made in the Introduction that the object of the foregoing analysis is to obtain an estimate of the contributions to the growth of a crack made by the differing forms of loading action - acoustic and pressurisation - both separately and in combination. The relative crack growth rates (i.e. crack growth per cycle) for the separate loading actions may simply be obtained from equations (8) and (11); however, bearing in mind the gross disparity in the frequency of application of stress

cycles which occur under the two forms of loading action, it is necessary to consider rather the relative contributions made to crack growth during a prescribed operational period.

Such an answer may be obtained by the use of equations (9) and (12) to evaluate relative crack growth under the two loading actions by introducing values of N_{ac} and N_p appropriate to the number of stress cycles occurring in the two cases during the period of operation. However, provided that the increment of crack growth in the period of operation is very small compared with the length of the crack at the start of the period, a simpler and adequate estimate may be made by multiplying the values of da/dN from equations (8) and (11) by the appropriate numbers of stress cycles. This proviso is met if the comparison of growth is made for one flight. Thus the increment of crack growth per flight under the acoustic loading Δa_{ac} closely approximates to:-

$$\Delta a_{ac} = C_1 C_2^n \lambda^n a^{n/2} (2\sigma^2)^{n/2} \Gamma_{x\to y}\left(\frac{n}{2} + 1\right) N_{ac} \qquad (14)$$

where N_{ac} is the number of stress cycles per flight under the acoustic loading spectrum, and a is the crack length at the start of the flight.

Since there is only one cycle of loading per flight associated with cabin pressurisation the corresponding increment of crack growth from this cycle, Δa_{pr}, is given (equation (11)) by:

$$\Delta a_{pr} = C_1 C_2^n a^{n/2} S_p^n \quad . \qquad (15)$$

The relative crack growth rate per flight under the two forms of loading action is given by:

$$\frac{\Delta a_{ac}}{\Delta a_{pr}} = \frac{\lambda^n (2\sigma^2)^{n/2} \Gamma_{x\to y}\left(\frac{n}{2} + 1\right) N_{ac}}{S_p^n} \quad . \qquad (16)$$

(At first sight it may appear from equation (16) that the relative crack growth rate is independent of crack length - this is not so in so far as the lower limit in the incomplete gamma function, $x = \frac{f_{th}^2}{2\sigma^2}$ is dependent on the crack length, a, for a given value of rms stress.)

Finally, an approximation to the increment of crack growth per flight under a combination of the two loading actions is given by:

$$\Delta a_{(pr+ac)} = C_1 C_2^n a^{n/2} \left[S_p^n + \lambda^n (2\sigma^2)^{n/2} \Gamma_{x \to y} \left(\frac{n}{2} + 1 \right) N_{ac} \right] \qquad (17)$$

and the relative crack growth rate (per flight) under the combined loading action and the cabin pressurisation alone is given by:

$$\frac{\Delta a_{(pr+ac)}}{\Delta a_{pr}} = 1 + \frac{\left[\lambda^n (2\sigma^2)^{n/2} \Gamma_{x \to y} \left(\frac{n}{2} + 1 \right) N_{ac} \right]}{S_p^n} \; . \qquad (18)$$

Before going on to apply the foregoing analysis to evaluate specific examples of crack behaviour under the differing forms of loading action, it is necessary to consider the probable value to be ascribed to the constant C_2.

The constant C_2 has been introduced into equation (2) to cover the effects that local structural constraints may have on the stress intensity at the crack tip: in the absence of such constraints it would be reasonable to ascribe a value of unity to C_2. Consideration of Fig.1 suggests that there are two types of constraint which should be considered in order to determine a modified value for C_2. Firstly considering the frames, which lie normal to the direction of crack growth, it would be reasonable to anticipate a correction factor based on the ratio of crack length to panel length (frame pitch) such that, for values of the ratio approaching unity, the rate of increase of stress intensity with increase in crack length would diminish as the frame accepted more load from the cracked panel. This effect has been quantified for in-plane loading by a number of investigators and it may be seen, for example, from the work of Isida[7] that the presence of the frame does not significantly affect the stress intensity at the crack tip until the ratio of crack length to frame pitch approaches 0.8. There is no reason to suppose that any proximity effect of the frame will have a greater effect on the value of the stress intensity in the reversed bending situation and for the range of values of crack length covered in the worked examples which follow (ratios of crack length to frame pitch <0.5), it is assumed that no allowance need be made for frame proximity in ascribing a value to the constant C_2. The second type of constraint which must be considered is that associated with the in-plane stiffness of the stringer which lies parallel to and close to the crack. In this

case, as far as the author is aware there is no specific solution to this configuration available on which to base an appropriate correction to the stress intensity at the crack tip. However, guidance may be obtained from the particular solution for a crack growing in a sheet with stringers of infinite in-plane stiffness attached symmetrically (back-to-back with the sheet between) and having the crack lying parallel to the stringers. It may be shown that, as such a crack is assumed to lie progressively closer to the stiffeners, the correction factor to crack tip stress intensity falls from a value of unity, at a distance, to a limiting value of 0.7 when the crack lies along the stiffener edge. In the case that we are considering, the in-plane stiffness of the stringer, taking it to be of conventional design, will be far from infinite - indeed it will be low in relation to the in-plane stiffness of the panel itself. Moreover the stringer is asymmetrically disposed about the plane of the panel. With these considerations in mind it is assumed that for both in-plane loading and/or bending the correction to the stress intensity factor will lie close to unity. Thus it is assumed that an overall value of unity may be taken for the constant C_2, for the panel geometry and crack length range considered, without the introduction of serious error.

5 APPLICATIONS OF THE ANALYSIS TO SPECIFIC CASES

In this section equation (18) is first evaluated, in order to illustrate the relative crack growth per flight under the cabin pressurisation alone and under a combination of both loading actions. Secondly, an equation is evaluated to illustrate typical (predicted) values of the increase in crack length between major inspection periods under the two forms of loading. These evaluations are carried out taking values of pressure cabin stress which typify those used in design, and for values of acoustic fatigue stress which fall within the range observed in structures which are satisfactory with respect to the acoustic loading alone. A range of crack lengths from 25 mm ($\approx$ 1 in) to 200 mm ($\approx$ 8 in) is covered.

The particular values of maximum stress in the pressure cabin which are considered are 70 MN m^{-2}, 85 MN m^{-2} and 100 MN m^{-2} ($\approx$ 10.2 ksi, 12.3 ksi and 14.5 ksi) - the range of values of acoustic fatigue stress lies between 5 MN m^{-2} and 10 MN m^{-2} rms ($\approx$ 0.725 ksi to 1.45 ksi, rms).

The material data used in the examples of this section are taken from the work of Hudson[5]. The material considered is 2024-T3 aluminium alloy sheet of thickness 2.25 mm (0.090 in) - average tensile properties are given in Table 2.

For this material Hudson quotes values of $C_1 = 1.04 \times 10^{-19}$, $m = 1.15$ and $p = 2.44$; n (which equals $m + p$) is taken as 3.6 in the analysis which follows.

5.1 Relative crack growth per flight under pressure cabin loading alone and the combination of acoustic and pressure cabin loading

The numerical results of the analysis, which are given in Table 3 and are presented in Fig.4, show the relative crack growth ratios per flight, $\Delta_{(pr+ac)}/\Delta_{pr}$, covering a range of acoustic fatigue stresses and cabin pressurisation stresses within the normal design range. It will be seen that over a considerable proportion of the range of acoustic stresses the crack growth rate from the combined loading exceeds that from cabin pressurisation alone by a large margin. For example, with a total crack length of 100 mm (≈ 4 in), a cabin pressurisation stress of 85 MN m^{-2} (≈ 12.3 ksi) and an acoustic fatigue stress of 8.75 MN m^{-2} (≈ 1.25 ksi), the rate of crack growth from the combined loading will be more than three times that from cabin pressurisation alone. The effect of crack length on the relative crack growth rate $\Delta_{(pr+ac)}/\Delta_{pr}$ is not very great as may be seen from Table 3. There is little variation (< 3%) of $\Delta_{(pr+ac)}/\Delta_{pr}$ for the range of crack length considered for acoustic fatigue stresses greater than 8.75 MN m^{-2} (≈ 1.25 ksi) rms - as the rms stress is reduced the variation in $\Delta_{(pr+ac)}/\Delta_{pr}$ with crack length becomes somewhat greater. (This may be understood in terms of an increasing number of acoustic stress cycles falling below the threshold f_{th} as discussed in section 4.2.)

5.2 Crack growth between major inspection periods, under pressure cabin loading alone and under the combination of acoustic and pressure cabin loading

An example to illustrate crack growth between major inspections - in this case assumed to take place every 3000 flights - has been taken, using equations (12) and (13). The results are given in Tables 4 and 5, respectively, and are presented in Fig.5. In this figure the crack growth arising from a combination of the two loading actions and from cabin pressurisation loading alone is shown for a range of initial crack lengths. It is seen, as would be anticipated from Fig.4, that the crack growth associated with the combined loading strongly predominates under the cabin pressurisation and the acoustic fatigue stresses considered; 85 MN m^{-2} and 8.75 MN m^{-2} rms (≈ 12.3 ksi and 1.25 ksi rms) respectively. For example, assuming a crack of 75 mm (total length) at the start of a major inspection period, the predictions indicate that the crack would grow a further 125 mm under the combined loading action as compared with a growth of 20 mm under the pressure cabin cycling alone.

6 CONCLUDING OBSERVATIONS

Consideration has been given in this Report to the relative contributions that acoustic loading and pressurisation cycling may make to crack growth in the pressure cabin of an aircraft. In particular, predictions have been made of the growth of a longitudinal crack lying close to a stiffener which forms one boundary of a fuselage panel, under the two forms of loading action. The results of the analysis have shown that the contribution to crack growth from the acoustic loding may exceed the contribution from pressurisation cycling by a considerable margin, even though the acoustic loading is not sufficiently severe to initiate fatigue damage in its own right. Thus, under a combination of both loading actions, which represents the situation which may obtain in service, the crack growth rate may be much faster than observed in the full scale fatigue test under cabin pressurisation alone. It may be necessary therefore to make allowance for the additional crack growth associated with any acoustic loading when establishing the fail safe characteristics of such structure.

Although the foregoing predictions have been limited to a study of crack behaviour in a pressure cabin the same considerations may also apply to other areas of structure which may be in an acoustic field, e.g. fin and tail plane structures, which may be designed on fail safe principles to withstand the appropriate gust and manoeuvre load fatigue spectra.

It should be borne in mind that a number of simplifying assumptions were made in the analysis and there is an evident need for experimental studies to substantiate the above predictions.

Appendix A

It is required to evaluate the integral $I = \int_0^\infty f^n P(f)df$, as in equation (6), where $P(f) = \frac{f}{\sigma^2} e^{-(f^2/2\sigma^2)}$.

Then
$$I = \frac{1}{\sigma^2} \int_0^\infty f^{(n+1)} e^{-(f^2/2\sigma^2)} df \quad . \tag{A-1}$$

Let
$$v = \frac{f^2}{2\sigma^2} \tag{A-2}$$

then
$$f^{(n+1)} = (2\sigma^2)^{(n+1)/2} v^{(n+1)/2} \tag{A-3}$$

and
$$df = \frac{\sigma^2}{(2\sigma^2 v)^{\frac{1}{2}}} dv \quad . \tag{A-4}$$

Substituting from (A-2), (A-3) and (A-4) in (A-1) gives

$$I = \frac{1}{\sigma^2} \int_0^\infty (2\sigma^2)^{(n+1)/2} v^{(n+1)/2} e^{-v} \frac{\sigma^2}{(2\sigma^2 v)^{\frac{1}{2}}} dv$$

therefore
$$I = (2\sigma^2)^{n/2} \int_0^\infty v^{n/2} e^{-v} dv \tag{A-5}$$

and, by definition, $\Gamma\left(\frac{n}{2} + 1\right) = \int_0^\infty v^{n/2} e^{-v} dv$

therefore (A-5) may be written

$$I = (2\sigma^2)^{n/2} \Gamma\left(\frac{n}{2} + 1\right) \quad . \tag{A-6}$$

Table 1

Values of $\Gamma_{x\to y}\left(\frac{n}{2}+1\right)$

f/σ	$\Gamma_{x\to y}\left(\frac{n}{2}+1\right)$	f/σ	$\Gamma_{x\to y}\left(\frac{n}{2}+1\right)$
0.0	1.6593	2.2	0.8788
0.2	1.6593	2.4	0.6706
0.4	1.6593	2.6	0.4970
0.6	1.6572	2.8	0.3590
0.8	1.6462	3.0	0.2244
1.0	1.6233	3.2	0.1532
1.2	1.5878	3.4	0.0757
1.4	1.4832	3.6	0.0389
1.6	1.3460	3.8	0.0162
1.8	1.1914	4.0	0.0000
2.0	1.0325		

Tabulated for $n = 3.6$ and upper bound $f/\sigma = 4$

f/σ, as given, refers to lower bound.

Table 2

The values of the material constants, C_1 and n_1 used in the analysis in this Report are based on crack propagation tests[5] on 2024-T3 aluminium alloy specimens having the following average tensile properties:-

Ultimate tensile stress	=	493 MN m^{-2} ($\approx$ 71.5 ksi)
Yield stress (0.2% off set)	=	356 MN m^{-2} ($\approx$ 51.6 ksi)
Percentage elongation (on 2 in)	=	21

Table 3

EVALUATION OF $\Delta ac/\Delta pr$ equation (18)

σ (MN m^{-2})	Total crack length, 2a (mm)	$\Delta_{(pr+ac)}/\Delta_{pr}$		
		S = 70 MN m^{-2}	S = 85 MN m^{-2}	S = 100 MN m^{-2}
5	25	1.518	1.257	1.143
5	50	1.613	1.304	1.169
5	100	1.635	1.315	1.175
5	200	1.639	1.317	1.176
6.25	25	2.273	1.631	1.351
6.25	50	2.394	1.691	1.385
6.25	100	2.424	1.706	1.393
6.25	200	2.426	1.707	1.394
7.5	25	3.626	2.302	1.726
7.5	50	3.721	2.349	1.752
7.5	100	3.739	2.358	1.757
7.5	200	3.745	2.360	1.759
8.75	25	5.602	3.281	2.272
8.75	50	5.696	3.328	2.298
8.75	100	5.702	3.332	2.300
8.75	200	5.702	3.332	2.300
10.0	25	7.783	4.363	2.875
10.0	50	7.830	4.386	2.888
10.0	100	7.838	4.390	2.890
10.0	200	7.838	4.390	2.890

Table 4

EVALUATION OF CRACK GROWTH UNDER CABIN PRESSURE CYCLING (equation (12))

Initial crack length (mm)	Growth/3000 flights (mm)
25	2.39
50	8.89
75	19.60
100	34.89

Table 5

EVALUATION OF CRACK GROWTH UNDER A COMBINATION OF BOTH LOADING ACTIONS (equation (13))

Initial crack length (mm)	Growth/3000 flights (mm)
25	9.73
50	45.01
75	130.81
100	343.72

SYMBOLS

a	crack length (2a total)	mm, in
C_1	material constant	
C_2	geometrical constant	
f	stress	MN m^{-2}, ksi
f_{th}	threshold stress	MN m^{-2}, ksi
k	stress intensity	MN $m^{-3/2}$, lb $in^{-3/2}$
m	material constant	
N	number of cycles	
N_{ac}	number of acoustic fatigue cycles	
p	material constant	
N_p	number of pressurisation cycles	
R	stress ratio (min/max) in fatigue cycle	
S_p	pressure cabin hoop stress (max)	MN m^{-2}, ksi
t	time	seconds
x,y	lower and upper bounds, respectively, of gamma function	
λ	constant	
Δa_{ac}	increment of crack growth under acoustic loading	mm
Δa_{pr}	increment of crack growth under pressure cabin cycle	mm
$\Delta a_{(pr+ac)}$	increment of crack growth under a combination of pressure cabin and acoustic loading	mm
σ	acoustic fatigue stress (root mean square)	MN m^{-2}, ksi
ω	natural frequency of panel	Hz

REFERENCES

No.	Author	Title, etc.
1	R.D.J. Maxwell	The practical implementation of fatigue requirements to military aircraft and helicopters in the United Kingdom - presented to the Sixth ICAF Symposium, Miami Beach, Florida, USA (1971)
2	-	Fatigue data sheets Nos. 66012, 67028, 72015. Published by the Engineering Sciences Data Unit Ltd., London.
3	F. Erdogan J.J. Kibler R. Roberts	Fatigue and fracture of thin-walled tubes containing cracks. First International Conference on pressure vessel technology, Delft (1969)
4	R. Roberts F. Erdogan	The effect of mean stress on fatigue crack propagation in plates under extension and bending. Journal of Basic Engineering, Vol.89, No.4, December 1967
5	C.M. Hudson	Effect of stress ratio on fatigue crack growth in 7075-T6 and 2024-TS aluminium alloy specimens. NASA TN D5390. August 1969
6	L.P. Pook	Fatigue crack growth data for various materials deduced from the fatigue lives of pre-cracked plates. NEL Report No.484 July (1971)
7	M. Isida	On the determination of stress intensity factors for some common structural problems. Engineering Fracture Mechanics, Vol.2, pp.61-79 (1970)

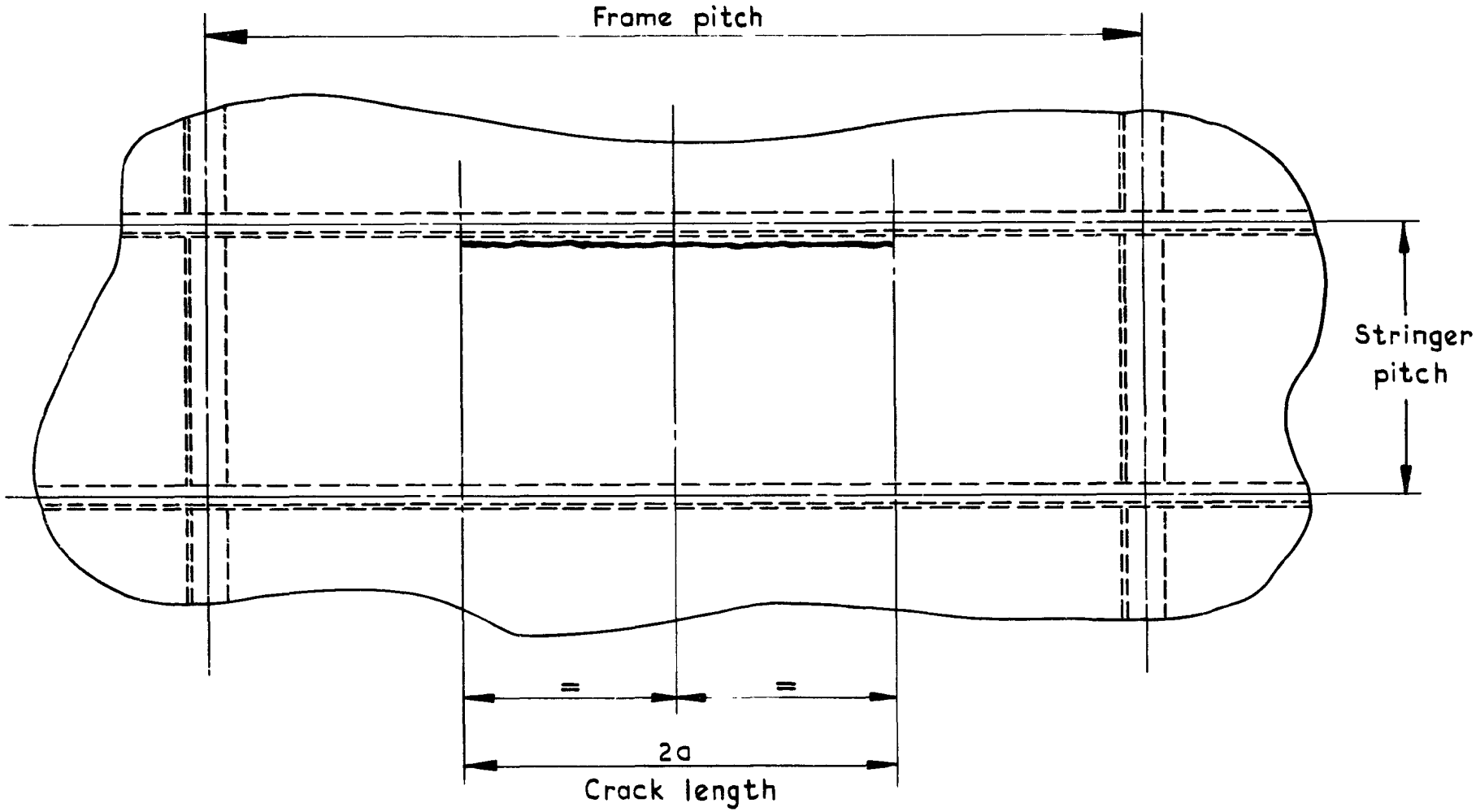

Fig.1 Fuselage panel showing crack running close to stringer edge

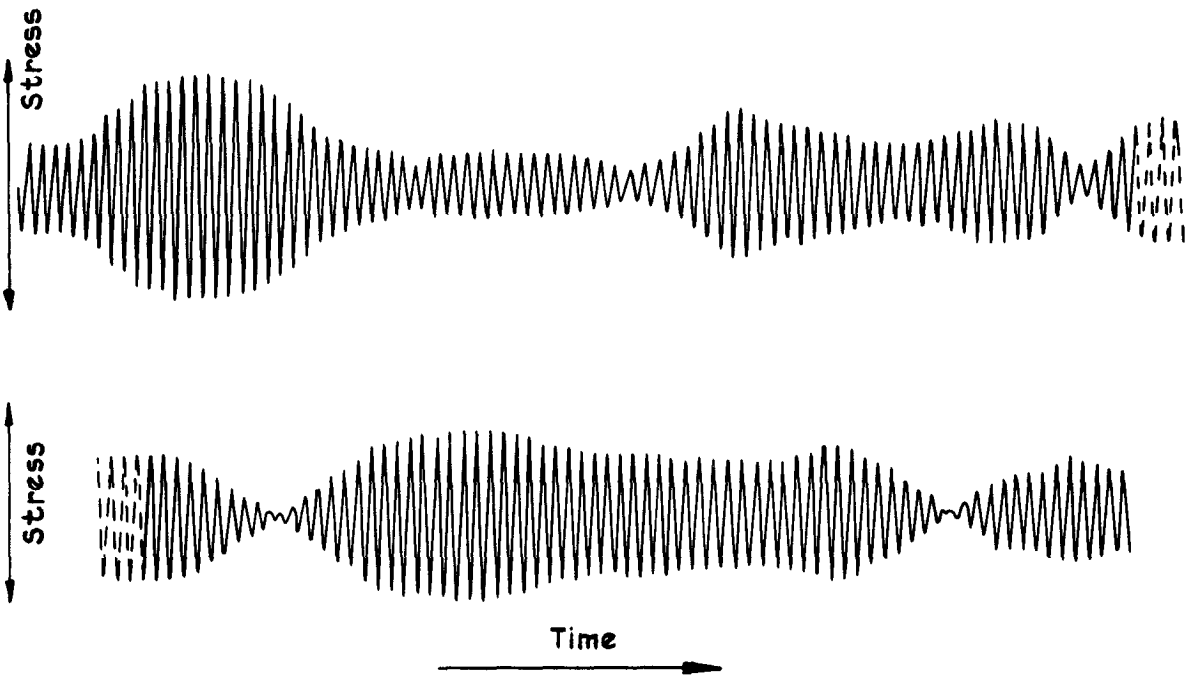

Fig. 2a Random stress - time waveform

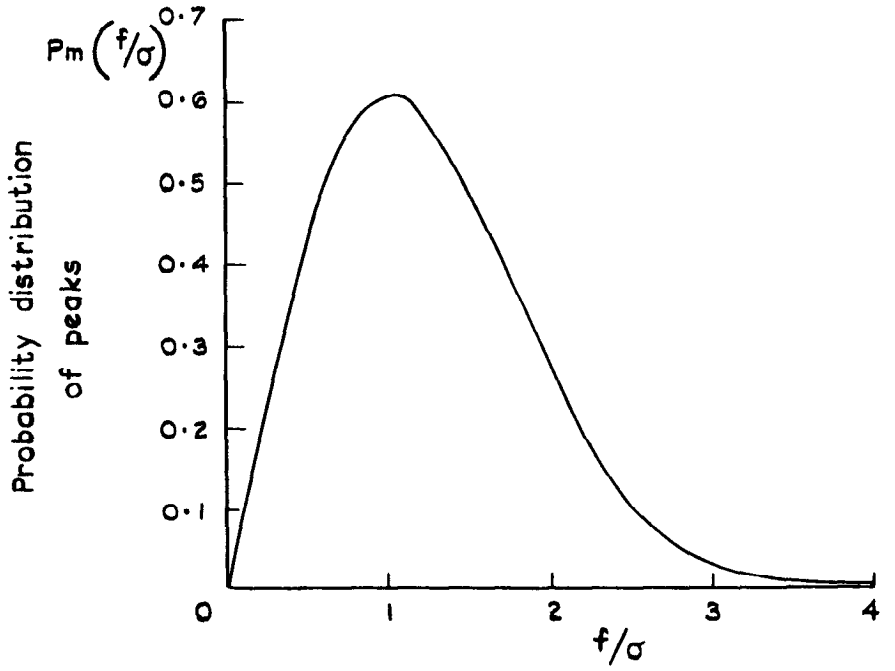

Fig. 2b Rayleigh distribution

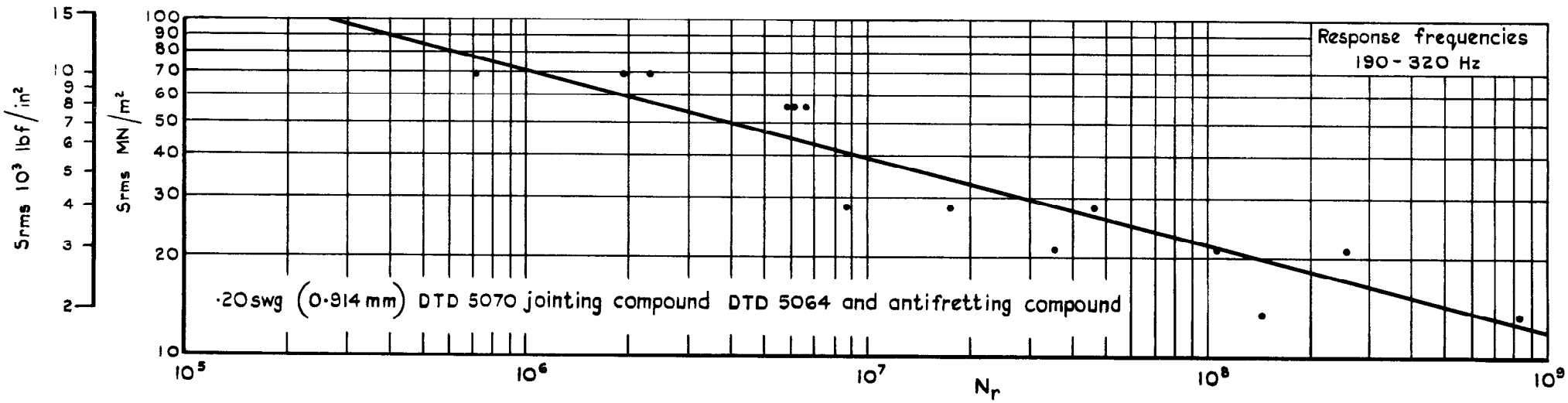

Fig. 3a S - N data for riveted skin – plain holes – type 1 viscoelastic jointing compound (from Ref 2)

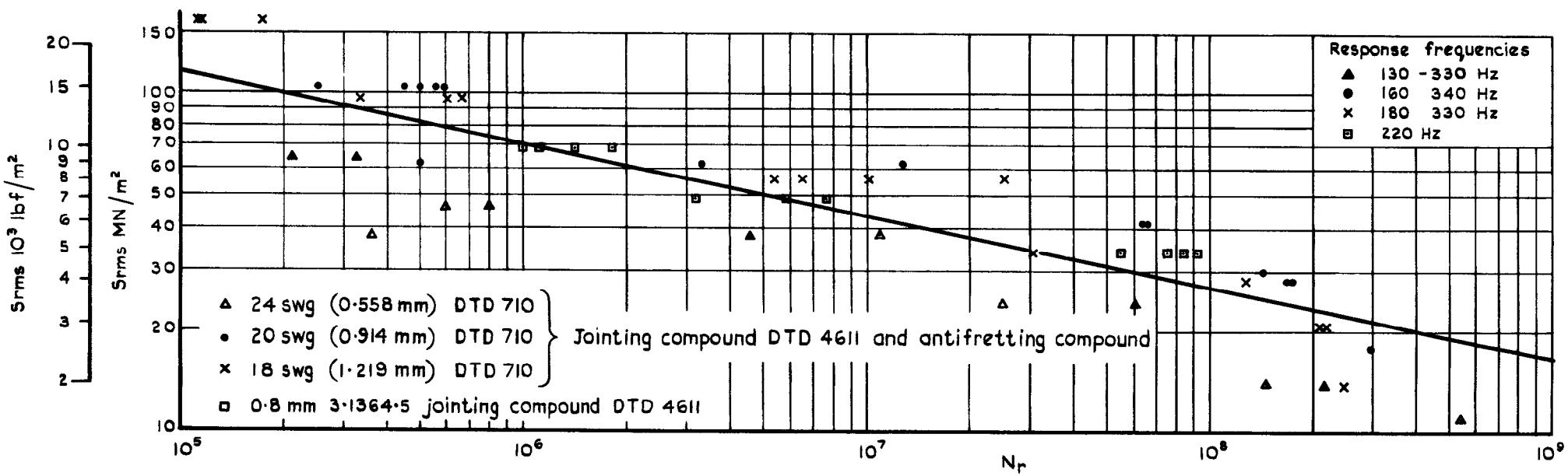

Fig. 3b S - N data for riveted skin – plain holes – type 2 viscoelastic jointing compound (from Ref 2)

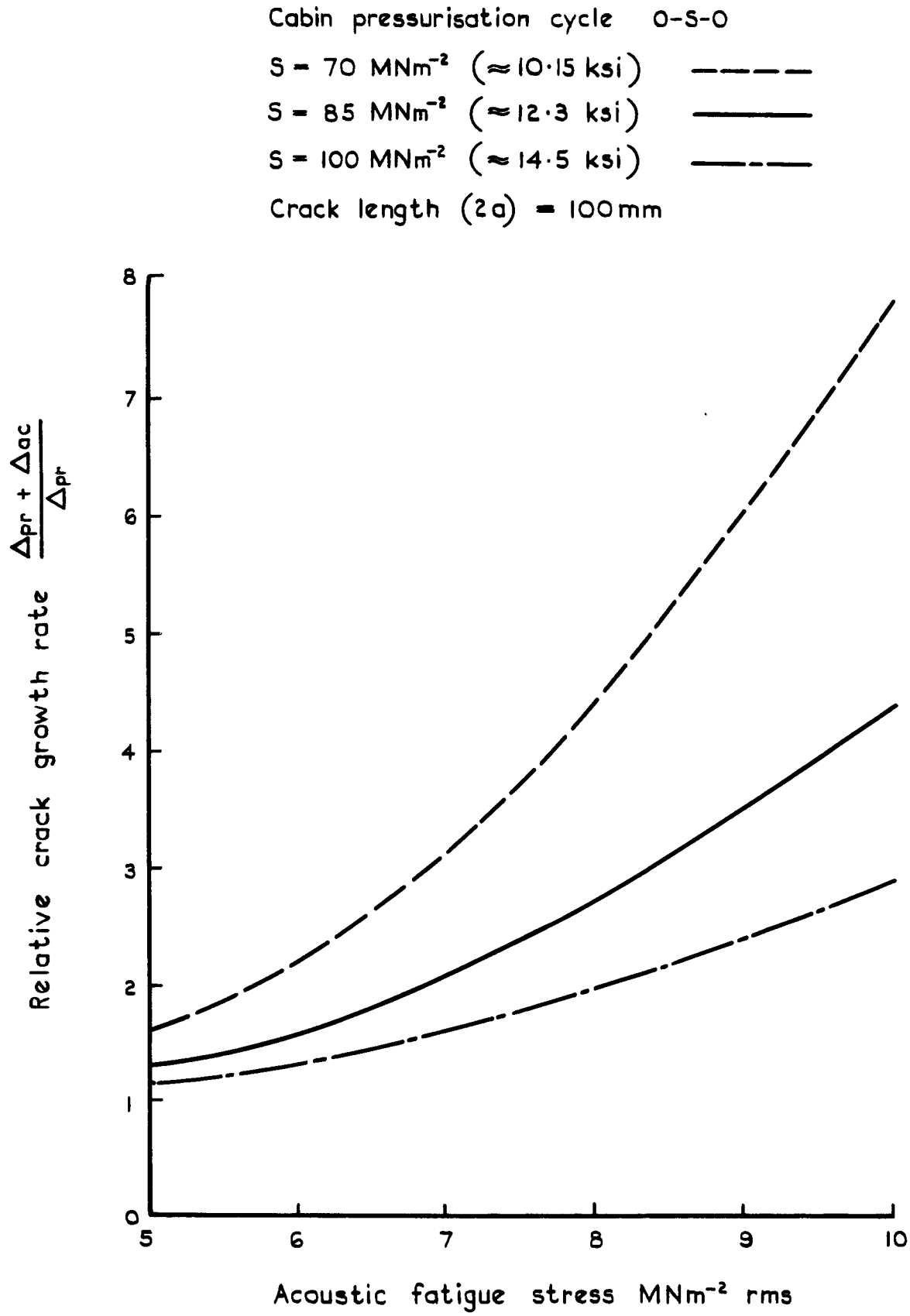

Fig.4 Relative crack growth rate per flight under pressurisation loading alone and under combined acoustic and pressurisation loading (eq 18)

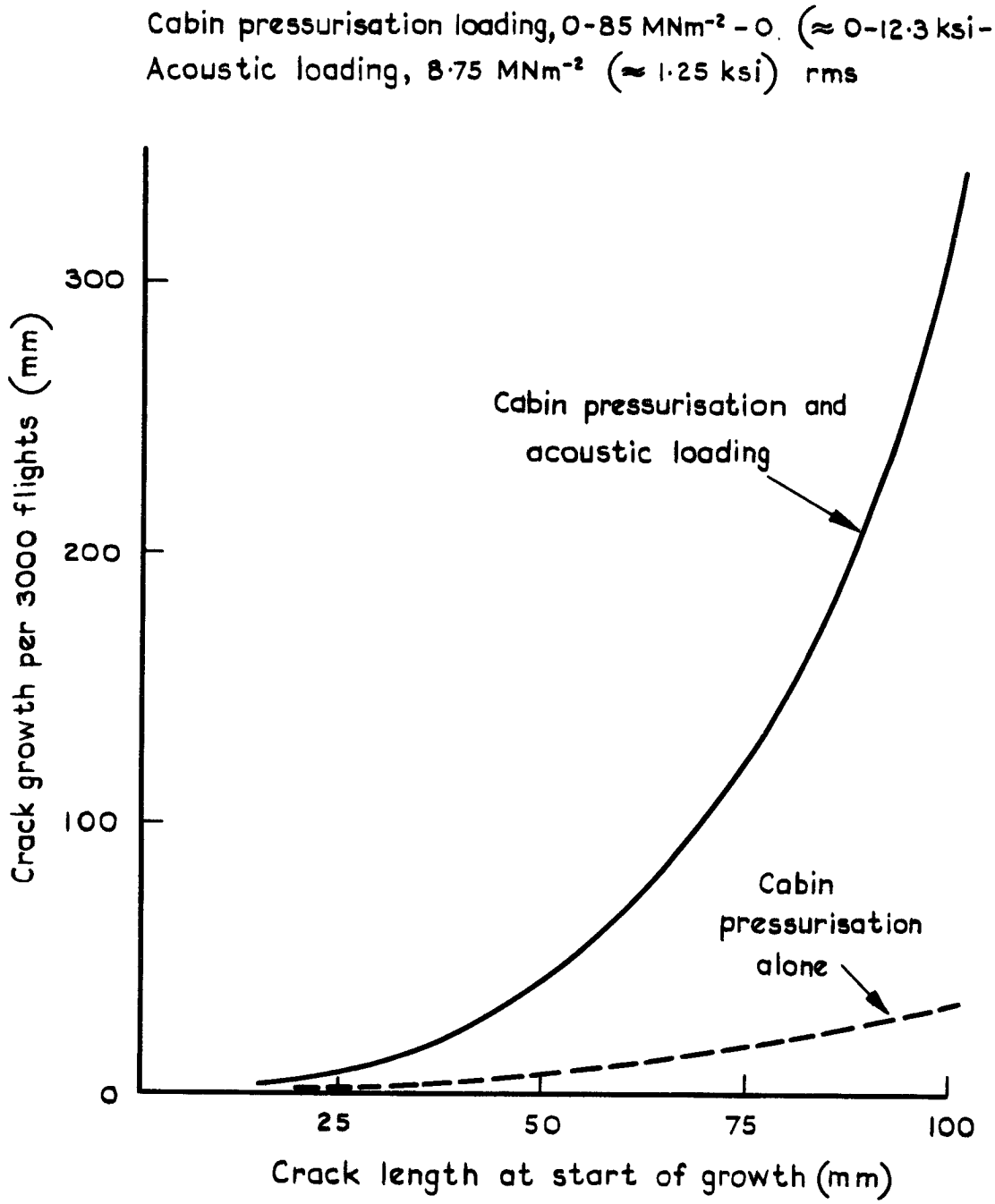

Fig. 5 Crack growth per 3000 flights arising from cabin pressurisation alone, and from combined pressurisation and acoustic loading (equations 12 & 13)

Printed in England for Her Majesty's Stationery Office by the Royal Aircraft Establishment, Farnborough Dd 505376 K4 4/74.

ARC CP No.1286
January 1973

Kirkby, W. T.

629.13.013.1/2 :
629.13.067.4 ·
539.219.2 :
539.831 :
539.433 :
534.1

SOME PREDICTIONS OF CRACK PROPAGATION UNDER COMBINED CABIN PRESURISATION AND ACOUSTIC LOADINGS

Predictions are made of the contributions that acoustic loading and pressurisation cycling may make to the growth of a longitudinal crack in the pressure cabin of an aircraft. The results of the analysis show that the contribution to crack growth from the acoustic loading may exceed the contribution from pressurisation cycling, even though the acoustic loading alone is not sufficiently severe to initiate fatigue damage.

It may be necessary therefore to make allowance for acoustic loading when establishing the fail safe characteristics of such structure and of other areas of structure where fail safe considerations apply.

Simplifying assumptions are made in the analysis and there is need for experimental studies to substantiate the above predictions.

Cut here

ARC CP No.1286
January 1973

Kirkby, W. T.

SOME PREDICTIONS OF CRACK PROPAGATION UNDER COMBINED CABIN PRESSURISATION AND ACOUSTIC LOADINGS

629.13.013.1/2
629.13.067.4
539.219.2 ·
539.831 ·
539.433
534.1

Predictions are made of the contributions that acoustic loading and pressurisation cycling may make to the growth of a longitudinal crack in the pressure cabin of an aircraft. The results of the analysis show that the contribution to crack growth from the acoustic loading may exceed the contribution from pressurisation cycling, even though the acoustic loading alone is not sufficiently severe to initiate fatigue damage.

It may be necessary therefore to make allowance for acoustic loading when establishing the fail safe characteristics of such structure and of other areas of structure where fail safe considerations apply.

Simplifying assumptions are made in the analysis and there is need for experimental studies to substantiate the above predictions.

Cut here

DETACHABLE ABSTRACT CARDS

DETACHABLE ABSTRACT CARDS

Published by
HER MAJESTY'S STATIONERY OFFICE

To be purchased from
49 High Holborn, London WC1V 6HB
13a Castle Street, Edinburgh EH2 3AR
41 The Hayes, Cardiff CF1 1JW
Brazennose Street, Manchester M60 8AS
Southey House, Wine Street, Bristol BS1 2BQ
258 Broad Street, Birmingham B1 2HE
80 Chichester Street, Belfast BT1 4JY
or through booksellers

C.P. No. 1286

ISBN 011 470870 3